JOURNAL OF MATERIALS SCIENCE 39 (2004) 833–838

Electrophoretic deposition of YSZ powders for solid oxide fuel cells

H. NEGISHI*, K. YAMAJI†, N. SAKAI†, T. HORITA†, H. YANAGISHITA*, H. YOKOKAWA†
*Research Institute for Green Technology and †Energy Electronics Institute, National Institute of Advanced Industrial Science and Technology (AIST), AIST Central 5-2, 1-1-1, Higashi, Tsukuba, Ibaraki 305-8565, Japan
E-mail: h-negishi@aist.go.jp

The technological feasibility of applying Electrophoretic Deposition (EPD) to Solid Oxide Fuel Cells (SOFCs) has been studied. Here, EPD characteristic of SOFC composition material powders has been investigated from the viewpoint of DC and AC electrochemical experiments. An electrolyte of SOFCs required gas tight dense coating. Commercial YSZ (3–8 mol% yttria stabilized zirconias) powders, as for the electrolyte materials, and various organic solvents were used in this study. In the case of 8YSZ (Tosoh, TZ-8Y) dispersed *n*-propanol bath, the zeta potential of 8YSZ particle showed positive and grain size distribution showed less than 0.1 μm. 8YSZ powder can be electrophoretically deposited onto the substrate because dispersed particle has charged and the charged particle acts as a migration onto the substrate by the potential gradient, and dense uniform coating was obtained less than 100 V/cm. On the other hand, as-deposited YSZ coating acts as a function of insulated layer. Potential gradient in the EPD bath has decreased because resistance of YSZ layer becomes higher than that of EPD bath with the progress of EPD under applied constant voltage. However, EPD bath characteristic itself does not change with the progress of EPD. It is suggested that the YSZ powder well dispersed EPD bath can be found by using 8YSZ and *n*-propanol.

1. Introduction

In recent years, many active investigations have been made to Solid Oxide Fuel Cells (SOFCs) because of the high-energy conversion efficiency and the excellent long-term stability [1]. Therefore, various processes have been adopted for fabricating the SOFCs. The wet-process fabrication is especially attractive because of the low cost and the mass productivity. For example, doctor-blade, screen printing and slurry coating technique have been extensively investigated. On the other hand, SOFCs can be adopted in many different stack designs. This is reasonable because of the use of all "solid" materials. Note that various different SOFC stack designs have been actually proposed and investigated so far [2]. However, there seem to be some difficulties in the conventional wet processes for the fabrication of SOFCs because of their complicated shape and size.

The electrophoretic deposition (EPD) process is very simple; the dispersed and charged particles in a solvent are migrated to an electrode substrate under some potential gradient with a DC power source. The EPD technique has some advantages compared with the other fabrication techniques especially on decreasing the fabrication costs and structural flexibility of single cells. The EPD technique was firstly proposed by Ishihara *et al*. for fabrication of SOFCs [3], and we applied this fabrication technique to cathode supported SOFCs [4].

We reported the technological feasibility of applying EPD technique to SOFCs investigated by making a porous LM/dense YSZ (yttria stabilized zirconia)/porous NiO-YSZ multilayers [4]. Dokiya *et al*. applied EPD on the anode substrate of Ni + YSZ which was prepared by reducing the substrate of Ni + YSZ [5]. Basu *et al* reported the uniform deposition of zirconia powders on a porous substrate by using a graphite interlayer approach [6]. Zhitomirsky *et al*. reported the EPD and electrolytic deposition of CeO_2 and $Ce_{1-x}Gd_xO_y$ films [7]. We also investigated to fabricate the anode-supported thin electrolyte films. In this case, 8YSZ powder was dispersed in a solvent of *n*-propanol with poly vinyl butyral (PVB), and was electrophoretically deposited onto the NiO-Scandia-stabilized Zirconia cermet substrate. Subsequently, the substrates and 8YSZ were co-fired. The thicknesses of the electrolytes were about 5–10 μm. The open circuit voltage value was almost equal to the theoretical value, which meant that the thin electrolyte was dense enough [8]. From these reports, it was considerably confirmed the feasibility of fabrication of thin YSZ electrolyte for SOFCs by EPD technique. On the other hand, to enhance the EPD techniques on fabrication of SOFCs, detail investigations of fundamental characteristic of EPD were required.

In this paper, we investigate the fundamental characteristic of EPD bath and function of deposition layer about YSZ electrolyte materials for SOFCs under applied constant voltage. For the preparation of YSZ powder well dispersed suspension, 3–8 mol% YSZ powders dispersion properties and zeta potential were investigated in various organic solvents without additions. Moreover, we investigated the EPD behavior from the viewpoints of current density, potential gradient and AC impedance analysis.

2. Experimental

YSZ powders for the electrolyte were commercial 3–8 mol% Y_2O_3 stabilized ZrO_2 powders (Tosoh, TZ-3Y, TZ-3YS, TZ-6Y, TZ-8Y and TZ-8YS, abbreviate at 3YSZ, 3YSZ(S), 6YSZ, 8YSZ and 8YSZ(S), respectively) with average particle size of about 0.3 μm. "S" means the "Slip casting" grade. EPD bath consisted of organic solvents and YSZ powders.

EPD bath were prepared as follows. YSZ powder was added into a solvent. The amount of powders was 0.125 g/50 cc. The powder in the solution was dispersed with ultrasonic vibration for 10 min and is kept over 48 h. Then, the precipitated powder was removed out of the solution. After the solution was dispersed again, the preparation of EPD bath was finished. EPD was operated with using a cell configuration as shown in Fig. 1. The deposition substrate was made from stainless steel (SUS304) wire. The counter electrode was made from stainless steel (SUS304) mesh or wire. The interval of both electrodes was ca. 10 mm. In the EPD process, DC voltage of 25–300 V was applied for 1–30 min with a regulated DC power supply (Takasago, TP0360-022D). Current density and potential were measured with a digital multimeter (Advantest, R6552). In the case of current density measurement, DC power source and multi-meter connected in series. In the case of potential measurement, one terminal of multi-meter connected deposition electrode for EPD and the other terminal connected platinum (Pt) probe. This Pt probe is placed between both electrodes in the EPD bath as shown in Fig. 1. For the point potential observation against deposition electrode, Pt probe is fixed. And for the potential gradient measurement, the probe is scanning between both electrodes. After EPD, the substrate that deposited YSZ powder was slowly dried up to avoid a formation of cracks during the drying process.

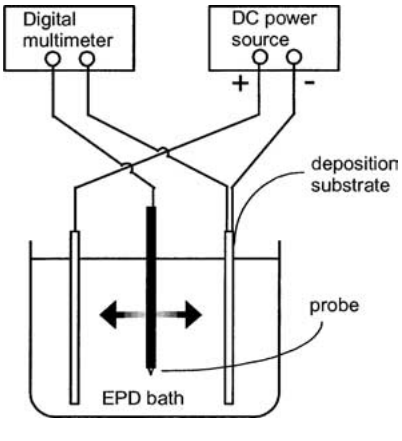

Figure 1 Cell configuration of EPD.

Particle size characterization was measured with a Coulter LS230. The zeta potential of YSZ particles was measured with an electrophoretic light scattering spectrophotometer (Otsuka electronics, ELS-8000). Microstructures of the deposited YSZ surfaces were observed with a scanning electron microscope (SEM, Hitachi, S800). The deposited sample was heat-treated at 1273 K for 1 h before the SEM observation. EPD bath characteristic and deposit coating resistibility in the EPD bath were measured with Impedance/Gain phase Analyzer (Solatron, SI-1260) and Electrochemical Interface (Solatron, SI-1287). Both electrode surface areas were 0.628 cm^2 respectively.

3. Results and discussion

3.1. Dispersion characteristic of YSZ powder in various organic solvents

Physical properties of promising organic solvents for the EPD bath are shown in Table I. The dielectric constant and viscosity data are very important for the EPD bath. The principle of the zeta potential measurement is expressed as:

$$U = V/E \tag{1}$$

$$\zeta = 4\pi\eta U/\varepsilon \tag{2}$$

where U is the electrophoretic mobility [m^2/s V], V is the velocity of particles [m/s], E is the applied potential [V/m], ζ is the zeta potential of particles [V], η is the viscosity of solvents [Ns/m^2] and ε is the dielectric constant [F/m]. Here, dielectric constant ε is the product of relative dielectric constant ε_r[−] and dielectric constant in vacuum ε_0 [F/m]. The dispersion characteristic and the zeta potential of the YSZ particles in various solvents were examined respectively. Each YSZ particle diameters before dispersion of each solvent are ca. 3 μm. The results of YSZ particles distribution after dispersed by using ultrasonic vibration are shown in Fig. 2. In the case of using acetone and acetylacetone, the suspensions are unstable. Particle distributions of Fig. 2g and h are appeared only in a few minutes after ultrasonic suspension. Moreover, condensation and sedimentation are easily observed with increasing of powder concentration without additions. Ishihara and we reported that the fabrication of YSZ by EPD using acetone [3, 4]. In these cases, iodine was added to the acetone because proton was produced with the reaction of iodine and acetone. Subsequently, YSZ particle had

TABLE I Physical properties of organic solvents [9]

Solvents	Viscosity (cP) (=10^{-3} N s m^{-2})	Relative dielectric constance (−)
Methanol	0.557	32.63
Ethanol	1.0885	24.55
n-propanol	1.9365	20.33
Iso-propanol	2.0439	19.92
n-butanol	2.5875	17.51
Ethylene glycol	16.265	37.7
Acetone	0.3087	20.7
Acetylacetone	1.09	25.7

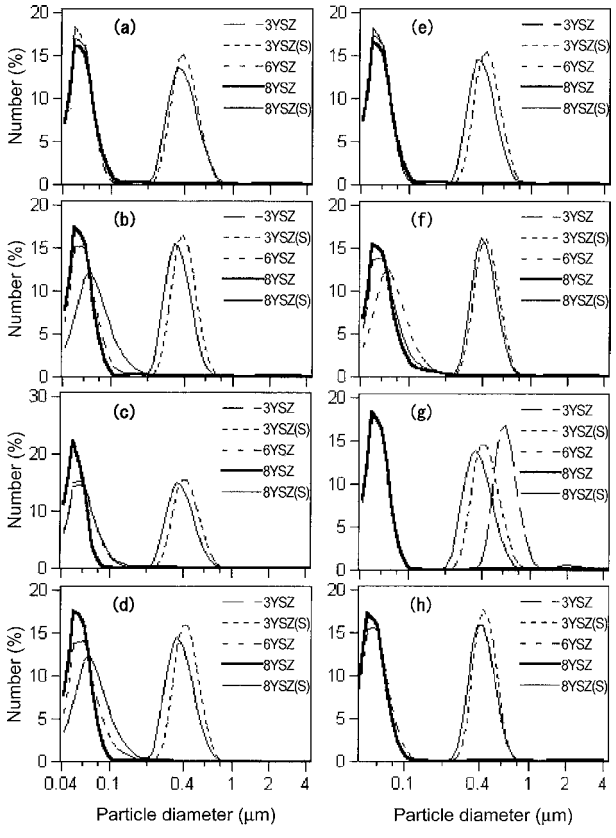

Figure 2 3–8 mol% YSZ powder distributions in various organic solvents: (a) methanol, (b) ethanol, (c) *n*-propanol, (d) iso-propanol, (e) *n*-butanol, (f) ethylene glycol, (g) acetone and (h) acetylacetone.

charged because of the created proton was adsorbed onto the YSZ particle. However, as we did not use an addition, dispersion property was different. On the other hand, each alcohol used for YSZ suspensions is stable. Particle diameters of 3YSZ, 6YSZ and 8YSZ show approximately less than 0.1 μm, and the 3YSZ(S) and 8YSZ(S) are distributed in the region of 0.2 to 0.8 μm in each alcohol as shown in Fig. 2. To prepare the well dispersed YSZ powder suspended EPD bath and to obtain a dense YSZ coating by EPD, it is considered that the suspension consisted of the fine particle will be better. For that reason, 3YSZ, 6YSZ and 8YSZ powder distribution with each alcohol solution show the excellent results. Especially the percentage of fine particle number of 8YSZ in *n*-propanol is relatively high.

Table II shows the zeta potentials of 3–8 mol% YSZ in each alcohol. Zeta potential of all combination shows positive. All combination can be adopted for the YSZ powder deposition by EPD technique. In the case of using ethylene glycol, the zeta potential is excellent however, the viscosity is high. It is considered that the 8YSZ powder suspended *n*-propanol bath has an excellent property from viewpoints of the powder distribution and the zeta potential.

TABLE II Zeta potentials of YSZ particles (mV)

Solvents	3YSZ	3YSZ(S)	6YSZ	8YSZ	8YSZ(S)
Methanol	1.68	0.52	0.72	0.67	0.57
Ethanol	1.31	5.80	1.22	1.96	1.94
n-propanol	1.57	5.49	5.69	8.13	2.64
Iso-propanol	4.23	3.98	1.19	4.30	3.06
n-butanol	20.55	24.41	8.00	5.23	9.57
Ethylene glycol	15.25	10.90	5.67	10.18	8.53

On the other hand, charging mechanism of YSZ particle can be considered as follows. The zeta potential showed high in the case of the large molecular weight of alcohol (e.g., *n*-butanol and iso-, *n*-propanol) as shown in Table II. The zeta potential of YSZ particles in various alcohols can be considered the same with our previous report, in which we reported the zeta potential about various kinds of oxide particles in various alcohols including a small amount of H_2O [10]. Commercial alcohols that we used in this study also include a small amount of H_2O. A small amount of H_2O in the alcohol generated H^+ ion and OH^- ion by electrolytic dissociation. This generated H^+ ion was adsorbed onto the oxide particle in an alcohol bath. It means that the zeta potential is influenced by the adsorption of H^+ ion onto the oxide in an alcohol bath because H^+ ion behaves as the potential determining ion. Amount of generated H^+ ion and adsorption behavior of H^+ ion on to the oxide particle depend on the kind of alcohol. The zeta potential in solvents tend to be in the order of *n*-butanol > iso-propanol > *n*-propanol > ethanol > methanol. This order is the same as the value of the relative dielectric constant. It is assumed that the H^+ ion tends to be adsorbed on the oxide in the alcohols relatively small dielectric constant, because the H^+ ion is difficult to exist in the high dielectric constant organic solvent.

3.2. EPD of 8YSZ in *n*-propanol suspension

Next, EPD property of 8YSZ powder suspended *n*-propanol bath was investigated. Fig. 3a shows the experimental result of the AC impedance analysis of powder free *n*-propanol and Fig. 3b shows the 8YSZ powder dispersed *n*-propanol bath. In the case of powder free *n*-propanol, a semicircle is observed (Fig. 3a). A semicircle of the starting point is the origin of the coordinate axes and the semicircle is the only one. Therefore, this only one resistance factor is caused by the *n*-propanol bath (Fig. 3a). This result shows good agreement with the case of applied high DC voltage. Fig. 4 shows the relationship between current density of YSZ powder free *n*-propanol and applied time as a function of applied DC voltages. It shows that the current density is comparably small to the applied high DC voltage to the *n*-propanol bath. The current densities are proportional with applied voltages and tend to unstable with highly applied DC voltages. It is considered that the unstable current density influences to the formation of uniform deposition during EPD of 8YSZ powder. Therefore,

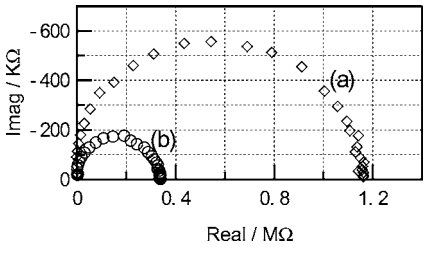

Figure 3 AC impedance diagram of: (a) YSZ powder free *n*-propanol and (b) YSZ powder dispersed *n*-propanol bath. Anode and Cathode: stainless steel wire (0.628 cm^2).

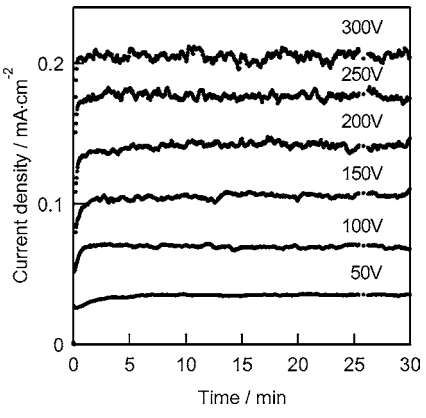

Figure 4 Relation between applied voltage and current density in *n*-propanol bath.

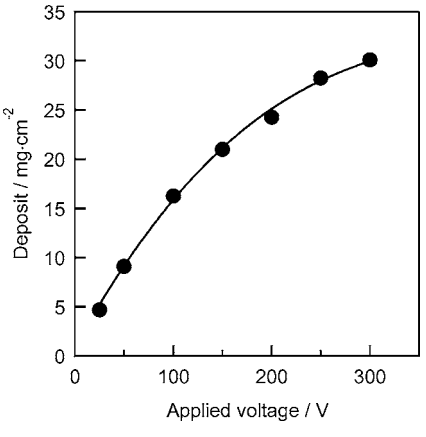

Figure 5 Relation between amount of deposit for 10 min and applied voltage.

it is suggested that the applied DC voltage should be less than 100 V in the case of *n*-propanol bath. On the other hand, after dispersed of 8YSZ powder, a semicircle becomes small as shown in Fig. 3b. A semicircle becoming small means decreasing of solution resistibility. From this result, it is obvious that the dispersed particle becomes charged and the charged particle acts a migration of electric charge.

Fig. 5 shows the amount of deposit as a function of applied voltages in the case of deposited for 10 min by using 8YSZ powder suspended *n*-propanol bath. 8YSZ particles were deposited on the cathode because the particle was charged positive. Amount of deposit increases with increasing of applied voltage. In the case of deposition at low voltages (e.g., 25 and 50 V), deposited YSZ coating surface morphologies are flat, but it will become rough with increasing of applied voltages. It is considered that one of these reasons is influenced by the unstable of current density. Fig. 6 shows SEM images of the deposited YSZ surface, which was deposited at 25, 50 and 100 V and subsequently pre-sintered at 1273 K for 1 h. YSZ was usually sintered at 1673 K for obtaining dense electrolyte layer. But here, the sample was pre-sintered at 1273 K to prevent shrink the deposition layer because for observation of the as-deposition morphology. In cases of deposited at 25 and 50 V, deposition surfaces were almost flat (Fig. 6a and b). On the other hand, deposited at 100 V, surface morphology was not flat (Fig. 6c). Therefore, it is suggested that the preparation of the uniform coating does not need high voltage. It can be obtained less than 100 V in the case of 8YSZ suspension *n*-propanol without additions.

Then, EPD characteristic less than 100 V was investigated. Fig. 7 shows the amount of deposit as a function of deposition time applied at 50 V. Amount of deposit increases and deposition rate becomes lower with increasing of deposition time. The current density decreases with increasing of deposition time as shown in Fig. 8. This is probably caused by the deposited layer that acts as a resistance layer, and the resistance increased by increasing amount of deposit. The potential change at 2 mm distance from the cathode during EPD was measured as shown in Fig. 9. The distance of both electrodes is 12.5 mm and applied voltage is 50 V (40 V/cm). In this case, Pt probe is fixed at 2 mm from deposition electrode. This point is close to the deposition electrode. Therefore, measurement potential is approximated potential drop in deposition layer. Observed potential was increased with increasing deposition time. This behavior is similar to the relation of amount of deposit and deposition time. On the other hand, difference between 50 V and measurement potential is approximated potential drop in EPD bath. It can

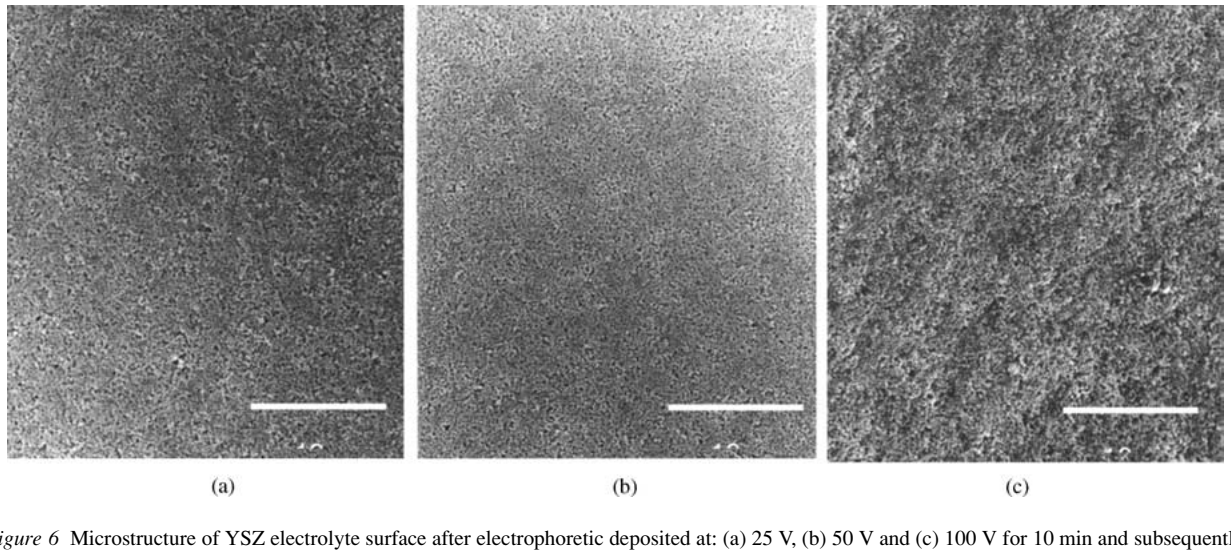

Figure 6 Microstructure of YSZ electrolyte surface after electrophoretic deposited at: (a) 25 V, (b) 50 V and (c) 100 V for 10 min and subsequently pre-calcined at 1273 K for 1 h.

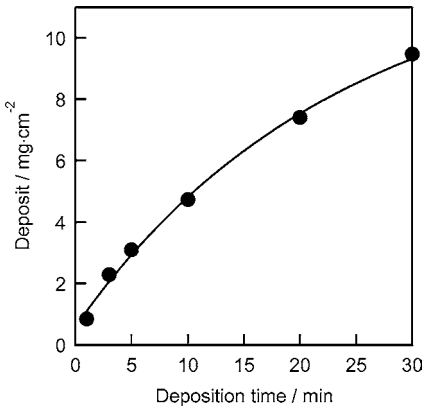

Figure 7 Relation between amount of deposit and deposition time at 50 V.

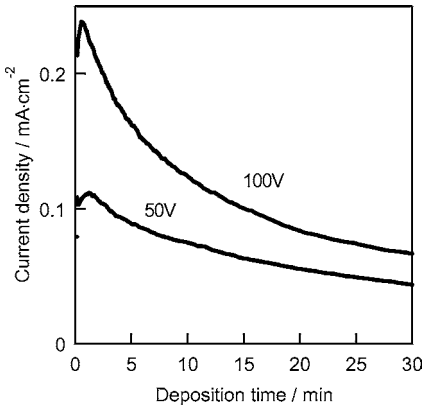

Figure 8 Relation between current density and deposition time.

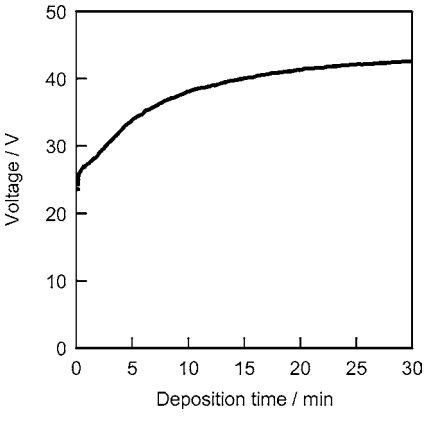

Figure 9 Potential changes at 2 mm from the deposition electrode when applied at 50 V.

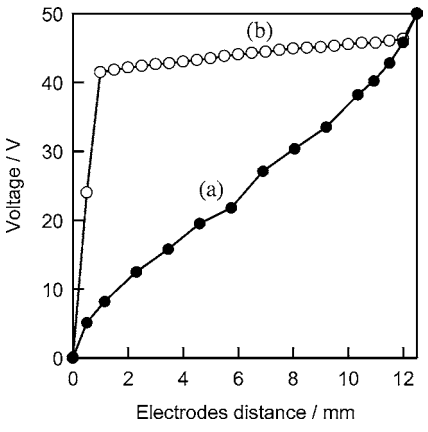

Figure 10 Potential gradients of: (a) powder free and (b) after 10 min deposited *n*-propanol bath when applied at 50 V.

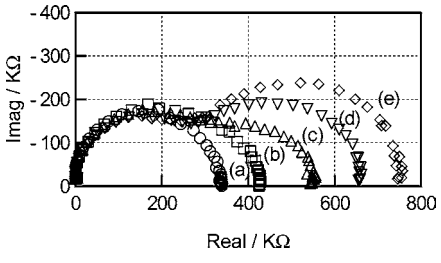

Figure 11 AC impedance diagram of YSZ powder coating on cathode in YSZ powder dispersed *n*-propanol bath deposit at 50 V. Anode and Cathode: stainless steel wire (0.628 cm^2): (a) 0 min, (b) 15 min, (c) 30 min, (d) 45 min and (e) 60 min.

be calculation of approximated potential gradient in the EPD bath, but it is not correct because potential drop of electric double layer between EPD bath/electrode interface is not considered. Therefore, potential gradient in the EPD bath was directly measured by scanning Pt probe. Fig. 10 shows the potential gradients between both electrodes of (a) 8YSZ powder free *n*-propanol bath and (b) after EPD of 8YSZ powder for 10 min. Potential gradient near the deposition substrate immediately changed according to make an 8YSZ deposit layer. It means that the resistance of deposition layer is much higher than that of EPD bath. These results also agreed with the formation of high resistance layer as described above. Fig. 11 shows the experimental result of the AC impedance analysis between both electrodes of 8YSZ powder dispersed *n*-propanol bath depends on the deposition time applied at 50 V. AC impedance analysis are measured each 15 min in interrupted in the EPD. In the progress of EPD, another semicircle appeared and became larger (from (b) to (e)). The first semicircle gives a resistance of EPD bath and this semicircle does not change with the progress of EPD. The second semicircle becomes large with the deposition time means the increasing of deposition coating thickness. Therefore, deposit layer acts a high resistance layer. This result shows good agreement with the result of DC potential measurements. Moreover, potential gradient in the bulk solution appears about 33 V/cm in the case of powder free bath. On the other hand, potential gradient after EPD of 8YSZ powder is about 4.3 V/cm. It means that the potential gradient is decreasing in the progress of EPD because of the formation of deposition layer as a high resistance layer. In addition, this resistance layer is increasing with increasing of deposition time as shown in Fig. 9. It means that the potential gradient in the EPD bath is decreasing with increasing of deposition time. Particle velocity V (m/s) is the product of electrophoretic mobility U (m^2/s V) and potential gradient E (V/m) from Equation 1. Therefore, decreasing of potential gradient means the decreasing of particle's velocity. From the result of potential gradient measurements, deposit layer resistance increases with increasing of deposition thickness and potential gradient becomes lower in the bulk EPD bath. As a result, deposition rate decreases with the progress of EPD.

However, bulk EPD bath characteristic itself does not change with the progress of EPD from AC impedance measurement. Here, we do not discuss the detail formation mechanism of deposit layer. But, these results by DC and AC electrochemical analysis contain useful information about deposit and provide powder onto the substrate.

Finally, it is found that the 8YSZ powder suspended *n*-propanol bath is useful and the bath's characteristic without addition can be obtained. We investigated and reported to fabricate the anode-supported thin electrolyte films for SOFCs [8]. In this report, 8YSZ powder dispersed *n*-propanol based bath was used. Here, NiO-Scandia-stabilized Zirconia cermet/8YSZ was prepared and open circuit voltage value was almost equal to the theoretical value at 1073 and 973 K, which meant that the thin electrolyte was dense enough. From these results, the feasibility of fabrication of thin YSZ electrolyte for SOFCs by EPD technique was considerably confirmed.

4. Conclusions

The fundamental characteristics of EPD about YSZ electrolyte materials for SOFCs were investigated. For the preparation of YSZ powder well dispersed suspension, 8 mol% YSZ powder suspended *n*-propanol bath was found out from the combination of 3–8 mol% YSZ and various alcohols. EPD characteristic to obtain the YSZ layer could be also cleared from the zeta potential, current density, potential gradient and AC impedance results. It is found that the resistibility of *n*-propanol bath has decreased by dispersing YSZ powder because dispersed particle becomes charged and the charged particle acts a migration of electric charge. In addition, deposit layer act as a resistance layer, but bulk EPD bath characteristic itself does not change with the progress of EPD. The present investigation has a role of enhancement for the technological feasibility of applying EPD technique to fabrication of SOFCs.

References

1. S. C. SINGHAL, in Solid Oxide Fuel Cells V, in Proceedings of the 5th International Symposium on Solid Oxide Fuel Cells, Aachen, June 1997, edited by U. Stimming, S. C. Singhal, H. Tagawa and W. Lehnert (The Electrochemical Society Series, NJ, 1997) PV 97-40, p. 37.
2. N. Q. MINH and T. TAKAHASHI, "Science and Technology of Ceramic Fuel Cells" (Elsevier, 1995).
3. T. ISHIHARA, K. SATO and Y. TAKITA, *J. Amer. Ceram. Soc.* **79** (1996) 913.
4. H. NEGISHI, N. SAKAI, K. YAMAJI, T. HORITA and Y. YOKOKAWA, *J. Electrochem. Soc.* **147** (2000) 1682.
5. T. N. LAN, K. KOBAYASHI, Z. CAI, I. TAKAHASHI, K. YAMAMOTO and M. DOKIYA, in Proceedings of the 7th International Symposium on Solid Oxide Fuel Cells, Tsukuba, June 2001, edited by H. Yokokawa and S. C. Singhal (The Electrochemical Society Series, NJ, 2001) PV2001-16, p. 1042.
6. R. N. BASU, C. A. RANDALL and M. J. MAYO, in Proceedings of the 6th International Symposium on Solid Oxide Fuel Cells, Hawaii, October 1999, edited by S. C. Singhal and M. Dokiya (The Electrochemical Society Series, NJ, 1999) PV99-19, p. 153.
7. I. ZHITOMIRSKY and A. PETRIC, in Proceedings of the 6th International Symposium on Solid Oxide Fuel Cells, Hawaii, October 1999, edited by S. C. Singhal and M. Dokiya (The Electrochemical Society, NJ, 1999) PV99-19, p. 217.
8. K. YAMAJI, H. NEGISHI, T. HORITA, N. SAKAI, Y. XIONG and H. YOKOKAWA, in Proceedings of the 5th European Solid Oxide Fuel Cell Forum, Switzerland, July 2002, edited by Joep Huijsmans (European Fuel Cell Forum, Switzerland, 2002) Vol. 1, p. 140.
9. KAGAKU BINRAN, "KISO-HEN" (Maruzen, Tokyo, 1975) [in Japanese].
10. Y. TAKAYAMA, H. NEGISHI, S. NAKAMURA, N. KOURA, Y. IDEMOTO and F. YAMAGUCHI, *J. Ceram. Soc. Jpn.* **107** (1999) 119.

Received 6 December 2002
and accepted 20 March 2003